World Electric Vehicle Journal

MDPI

Article

Electrical Interoperability Evaluating of Wireless Electric Vehicle Charging Systems Based on Impedance Space

Bingkun Shi [1], Fuyuan Yang [1,*], Bin Wei [2] and Minggao Ouyang [1]

[1] State Key Laboratory of Automotive Safety and Energy, Tsinghua University, Beijing 100084, China; sbk17@mails.tsinghua.edu.cn (B.S.); ouymg@tsinghua.edu.cn (M.O.)
[2] China Electric Power Research Institute, State Grid Corporation of China, Beijing 100192, China; weibin@epri.sgcc.com.cn
* Correspondence: fyyang@tsinghua.edu.cn

Abstract: In the commercialization process of wireless electric vehicle charging (WEVC), it is essential to ensure the interoperability between diverse WEVC systems due to the wide application of various coil configurations and compensation topologies. This paper proposes a novel electrical interoperability evaluation method based on impedance indices and corresponding feasible space in the complex plane. Firstly, the electromagnetic description of the coil system is introduced to reveal the energy flow process of WEVC system. Further, two key impedance indices and their feasible space are derived and verified. Interoperability evaluation results show that the reference devices in Chinese WEVC standard GB/T 38775.6 and GB/T 38775.7 are able to achieve the requirements of power capability. Moreover, it is necessary to reduce the duty cycle of rectifier when the battery voltage rises so as to narrow down the variation of load resistance and avoid dangerous working conditions. The proposed method can effectively evaluate the electrical interoperability of WEVC systems from different manufacturers under different power or distance levels before conducting experiments.

Keywords: electric vehicle; wireless power transfer; system interoperability; circuit impedance

check for updates

Citation: Shi, B.; Yang, F.; Wei, B.; Ouyang, M. Electrical Interoperability Evaluating of Wireless Electric Vehicle Charging Systems Based on Impedance Space. *World Electr. Veh. J.* **2021**, *12*, 245. https://doi.org/10.3390/wevj12040245

Academic Editor: Peter Van den Bossche

Received: 19 October 2021
Accepted: 11 November 2021
Published: 16 November 2021

Publisher's Note: MDPI stays neutral with regard to jurisdictional claims in published maps and institutional affiliations.

Copyright: © 2021 by the authors. Licensee MDPI, Basel, Switzerland. This article is an open access article distributed under the terms and conditions of the Creative Commons Attribution (CC BY) license (https://creativecommons.org/licenses/by/4.0/).

1. Introduction

Wireless electric vehicle charging (WEVC) is stepping onto the stage of commercialization. However, in order to promote the progress of WEVC technology, it is necessary to maintain the diversity of product designs. Currently, there are many well-established coil configurations and compensation topologies for WEVC system [1].

Interoperability of WEVC means that ground assemblies (GA) and vehicle assemblies (VA) produced by different WEVC manufacturers can transmit power and meet the performance and functional requirements. It also implies that systems under different power and ground clearance levels should operate with each other in accordance with certain rules. Tables 1 and 2 show the definition and interoperability requirements of power levels and ground clearance levels in exposure drafts of Chinese GB/T standard [2–5].

The magnetic coupling system (i.e., coil system) and compensation circuit are two key components of WEVC systems. As a result, magnetic interoperability and electrical interoperability are proposed in international standards such as SAE J2954 [6]. This paper focuses on electrical interoperability, which means that the compensation networks of GA and VA should work well with each other and meet the power and efficiency requirement.

Figure 1 summarizes the interoperability for different compensation topologies in literatures [7–13]. As a topology with remarkable performance, the interoperability between LCC topology and other topologies receives extensive attention. Ali Ramezani et al. analyzed the LCC-S topology in the time domain and pointed out that the topology has the characteristics of output constant voltage and can realize zero voltage switching [10]. Ruikun Mai et al. analyzed the S-LCC topology and proved that it can realize weak communication control and input zero phase angle [11]. In addition, interoperation experiments

on LCC compensation and Parallel compensation are carried out and the results show that all combinations of LCC and Parallel can achieve power and efficiency requirements [12,13]. However, these studies apply different evaluation methods and criteria, and even different circuit structures, which makes it difficult to get a general conclusion.

Table 1. Interoperability requirements for different power levels.

	GA: WPT1	GA: WPT2	GA: WPT3
VA: WPT1	3.7 kW	3.7 kW	3.7 kW
VA: WPT2	3.7 kW	7.7 kW	7.7 kW
VA: WPT3	3.7 kW	7.7 kW	11.1 kW

Table 2. Interoperability requirements for different ground clearance levels.

	GA: Z1(100–150 mm)	GA: Z2(100–210 mm)	GA: Z3(100–250 mm)
VA: Z1(100–150 mm)	Supported	Supported	Supported
VA: Z2(140–210 mm)	Not supported	Supported	Supported
VA: Z3(170–250 mm)	Not supported	Not supported	Supported

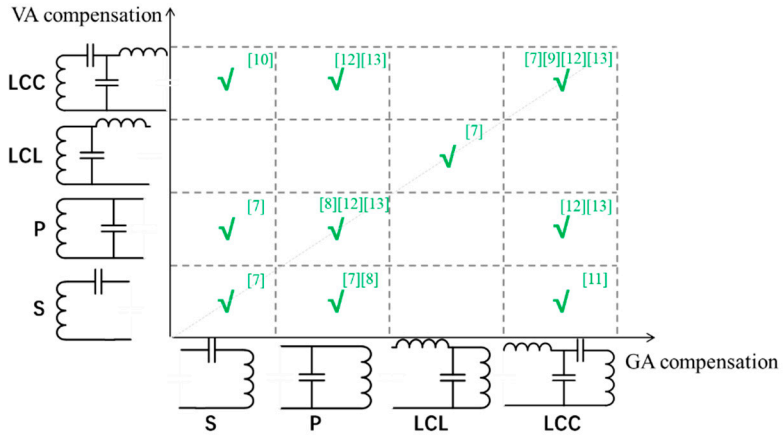

Figure 1. Interoperability for different GA and VA compensation.

To describe the electrical interoperability, the VA side impedance Z_{VA} and the GA side impedance Z_{GA} are defined in SAE J2954, as presented in Figure 2. Several recommended parameters for GA side impedance are derived based on the performance of reference devices. The analysis in the SAE standard is of great value for the evaluation and optimization of interoperability. Nevertheless, it cannot reflect the influence of circuit constraints (such as coil current, DC input voltage) on electrical interoperability.

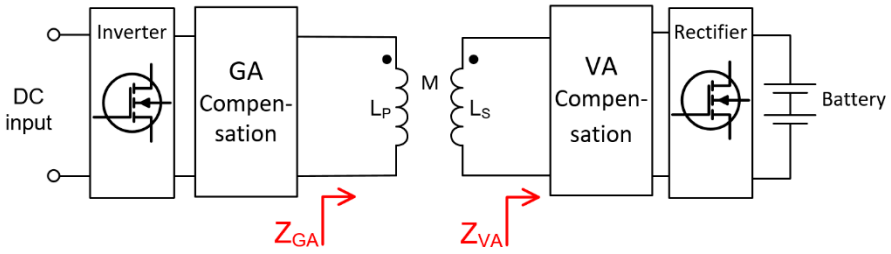

Figure 2. Definition of Z_{GA} and Z_{VA} in SAE J2954.

This paper proposes a novel electrical interoperability evaluation method based on impedance analysis. Current and voltage limits of key components are transformed into constraints of circuit impedance parameters, and consequently, the power capability of

the system can be evaluated by inclusion relationship between the feasible impedance space and operating impedance points. The method is based on a general circuit model for WEVC system so it can be applied to various circuit topologies with a very small amount of calculation.

The paper is organized as follows. Section 2 introduces the electromagnetic description of a coil system and derives the power equation of WEVC system. In Section 3, key impedance indices and their feasible space are proposed to describe electrical interoperability. The method is applied and validated based on a set of interoperability experiments in Section 4. Finally, some conclusions and discussions are summarized in Section 5.

2. Electromagnetic Description of Coil System

This section discusses the essence of a coil system from the perspective of electromagnetism. No matter what coil configuration and compensation topology are used in a wireless charging circuit, the coil system can be regarded as a storage and transmission system of electromagnetic energy, as shown in Figure 3. This is a two-port system, and energy can flow into or out of the system via the two ports. When neglecting the coil loss, the power flow of the system at arbitrary time is described as below.

$$P_1 + P_2 = \frac{dW_{mag}}{dt}. \tag{1}$$

P_1 and P_2 mean the power flow at port 1 and port 2. If the power flows into the system from port 1, P_1 is positive, otherwise it is negative. The same rule applies to port 2. W_{mag} refers to the magnetic energy stored in the system, and $\mathrm{d}W_{\mathrm{mag}}/\mathrm{d}t$ shows the change rate of magnetic energy.

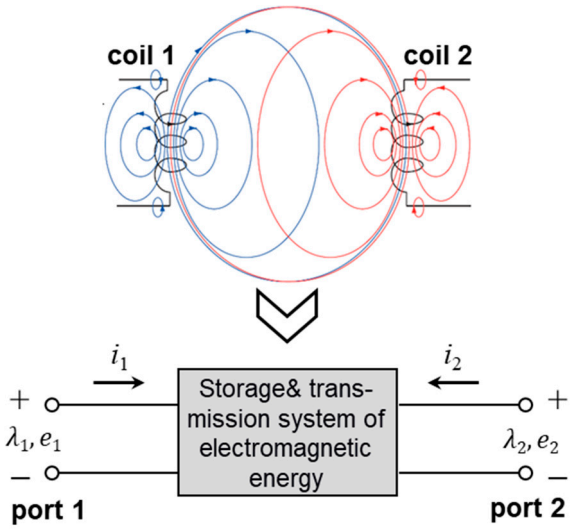

Figure 3. The essence of coil system from the perspective of electromagnetism.

Regarding the coil currents i_1, i_2 as state variables, the state equations of the system can be derived according to the electromagnetism.

Firstly, flux linkage equations are

$$\lambda_1 = L_1 i_1 + M i_2,\ \lambda_2 = L_2 i_2 + M i_1, \tag{2}$$

where λ_1, λ_2 are the magnetic fluxes of coil 1 and coil 2, L_1, L_2 are self-inductances, and M is mutual inductance between the two coils.

Secondly, electricity and magnetism are connected by Faraday's law:

$$e_1 = \frac{d\lambda_1}{dt},\ e_2 = \frac{d\lambda_2}{dt}, \tag{3}$$

where e_1, e_2 are the voltages at port 1 and port 2.

The last state equation is a variant of Equation (1):

$$dW_{mag} = e_1 i_1 dt + e_2 i_2 dt. \tag{4}$$

Combining Equations (2)–(4), we can obtain the following expression:

$$\begin{aligned} dW_{mag} &= e_1 i_1 dt + e_2 i_2 dt \\ &= i_1 d\lambda_1 + i_2 d\lambda_2 \\ &= L_1 i_1 di_1 + L_2 i_2 di_2 + M i_1 di_2 + M i_2 di_1 \end{aligned} \tag{5}$$

Integrating the above equation, we can get magnetic energy stored in the coil system:

$$W_{mag} = \frac{1}{2} L_1 i_1^2 + \frac{1}{2} L_2 i_2^2 + M i_1 i_2. \tag{6}$$

In W_{mag}, $\frac{1}{2} L_1 i_1^2$ and $\frac{1}{2} L_2 i_2^2$ are the energy of the self-induced flux in coil 1 and coil 2, respectively. These two parts of energy only flow back and forth on one side, but not to the other side. $M i_1 i_2$ is the energy of a mutual induced flux, which can flow from one side to the other, as shown in Figure 4. In a current cycle, when port 1 inputs energy to the coil system, port 2 outputs energy from the coil system (or vice versa).

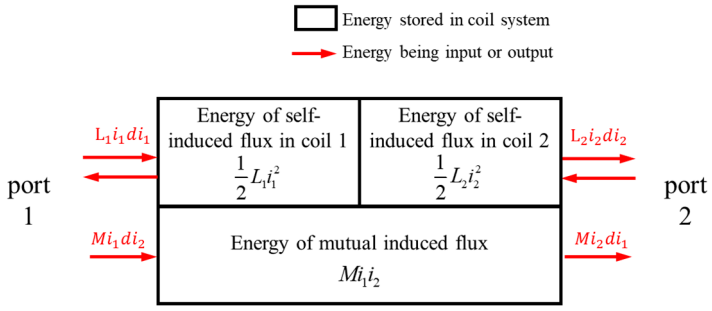

Figure 4. Composition of energy stored in coil system and energy flow.

Suppose that i_1 and i_2 are alternating currents with a phase difference φ_{12}:

$$i_1 = \sqrt{2} I_1 \sin(\omega t),\ i_2 = \sqrt{2} I_2 \sin(\omega t - \varphi_{12}), \tag{7}$$

where I_1, I_2 are the effective values of i_1, i_2 and ω is the angular frequency. In one current cycle, the energy transferred from port 1 to port 2 is:

$$\begin{aligned} &\oint Mi_1 di_2 = -\oint Mi_2 di_1 \\ &= \tfrac{1}{2} \oint (Mi_1 di_2 - Mi_2 di_1) \\ &= 2\pi M I_1 I_2 sin\varphi_{12}. \end{aligned} \tag{8}$$

Therefore, the transmission power of any coil system can be expressed as:

$$P_{1\to 2} = f \cdot 2\pi M I_1 I_2 \sin\varphi_{12} = \omega M I_1 I_2 \sin\varphi_{12}. \tag{9}$$

According to Equation (9), the determinants of transmission power are summarized as follows. (a) Coil current angular frequency ω, higher frequency can help achieve higher power density. (b) Mutual inductance M, which reflects the magnetic coupling characteristics between the coils. (c) Effective values of coil currents I_1, I_2, which reflect the power capacity of coils, compensation network and other power electronics on both sides. (d) Phase difference φ_{12} of coil currents, which reflects the degree of mutual induced energy transformed into effective transmission energy. When $\varphi_{12} = \pm 90^\circ$, all the energy input from one port can output into the other port (the direction of energy flow depends

on the sign of φ_{12}). Otherwise, there will be some energy backflow, which means that the power transmission capacity declines, as shown in Figure 5. Compared with an ideal situation φ_{12} = 90°, the power capacity is reduced by 13%, 29%, in the case of φ_{12} = 60°, 45°, and 30°, respectively.

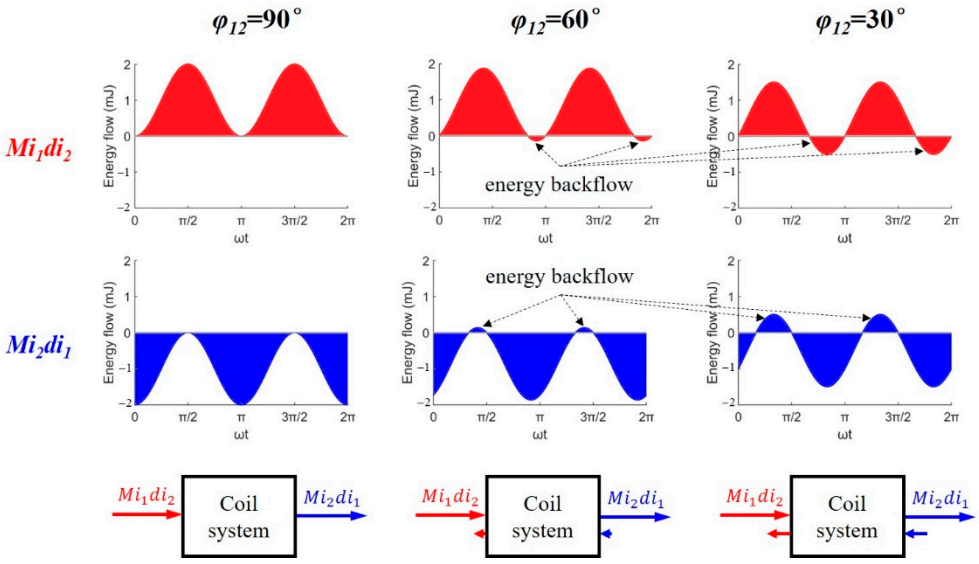

Figure 5. Energy flow at different φ_{12} in a current cycle (M = 10 μH, I_1 = 10 A, I_2 = 10 A).

3. Evaluation Indices of Electrical Interoperability

3.1. Definition of Key Impedance

With the help of circuit theory, the interoperability of WEVC system can be further evaluated. Figure 6 sketches a universal WEVC circuit model, including voltage source, coil system, compensation networks, and battery load. L_P, L_S, and M are self-inductance of GA coil, self-inductance of VA coil, and their mutual inductance. The model adopts the T-type equivalent circuit of mutual inductance to realize a decoupled connection of GA and VA circuits. In addition to the design of coils on both sides, coil inductance parameters {L_P, L_S, M} are also affected by the relative position between the coils. As a result, compensation networks are introduced into both sides of charging system so as to compensate the reactive power generated by coil system.

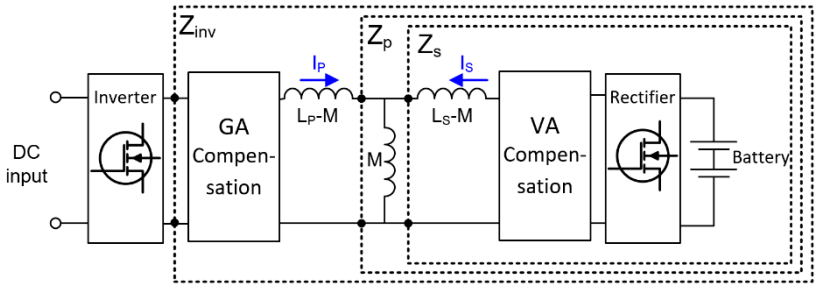

Figure 6. Circuit model and impedance definition of WEVC system.

Therefore, impedance is the key to analysing the power flow in WEVC circuit, and it is also an important indicator for judging the interoperability between GA and VA. A GA-VA pair which achieves interoperability means that the circuit impedance is controlled within a reasonable range under all possible charging conditions and possible coil inductance parameters {L_P, L_S, M}, so that power electronics will not exceed their safe operating area.

As indicated in Figure 6, Z_S, Z_P, and Z_{inv} are the three key impedances. Z_S includes the load, VA compensation network, and decoupled VA coil (i.e., L_S-M). On the basis of Z_S

range, Z_P includes mutual inductance branch additionally. Z_{inv} is the input impedance of the inverter, including GA compensation network, coil system and the whole VA circuit.

3.2. Interoperability Evaluation Index I: Z_{inv}

The role of Z_{inv} is to convert a safe operating area of the inverter into a safe impedance area of the circuit. Assume that the maximum voltage and current of the inverter are U_{inv_max} and I_{inv_max}, respectively.

$$|U_{inv}| \le U_{inv_max},\ |I_{inv}| \le I_{inv_max}. \tag{10}$$

According to Ohm's law of AC circuit,

$$\dot{U}_{inv} = \dot{I}_{inv} Z_{inv}. \tag{11}$$

The input power can be expressed as

$$P_{in} = \dot{U}_{inv} \cdot \dot{I}_{inv} = |I_{inv}|^2 |Z_{inv}| \cos\varphi(Z_{inv}) = \frac{|U_{inv}|^2 \cos\varphi(Z_{inv})}{|Z_{inv}|}. \tag{12}$$

where $|Z_{inv}|$ and $\varphi(Z_{inv})$ are the amplitude and phase of the impedance Z_{inv}.

From Equations (10) and (12), the amplitude constraints of Z_{inv} are derived:

$$\max|Z_{inv}| = \frac{U_{inv_max}^2 \cos\varphi(Z_{inv})}{P_{in}},\ \min|Z_{inv}| = \frac{P_{in}}{I_{inv_max}^2 \cos\varphi(Z_{inv})}. \tag{13}$$

In addition, in order to ensure the soft switching operation of the inverter, the phase of U_{inv} is generally required to be ahead of I_{inv}, which is essentially a constraint of $\varphi(Z_{inv})$.

$$\varphi\left(\dot{U}_{inv}\right) - \varphi\left(\dot{I}_{inv}\right) = \varphi(Z_{inv}) > 0. \tag{14}$$

With the help of the Z_{inv} amplitude constraints (13) and Z_{inv} phase constraint (14), feasible impedance space of Z_{inv} can be determined, and it can be transformed into a complex plane, as shown in Figure 7.

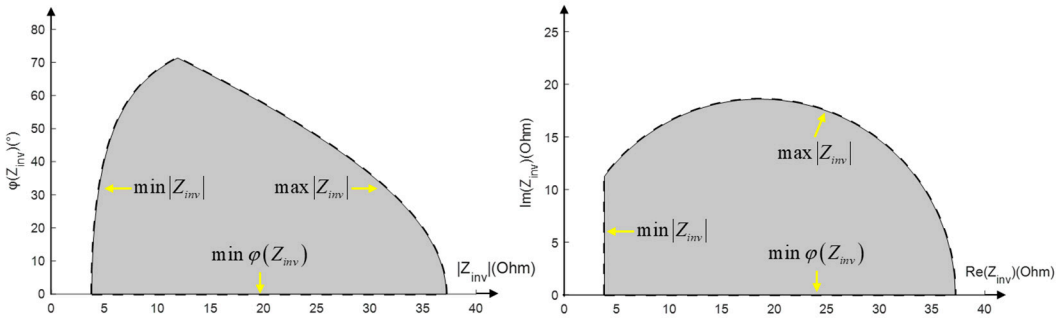

a) Amplitude-phase plane of Z_{inv} b) Complex plane of Z_{inv}

Figure 7. An example of feasible Z_{inv} space.

Figure 8 explains the steps of interoperability evaluation using the impedance index Z_{inv}. Note that Z_{inv} is merely one of the evaluation indices, and it mainly evaluates the power capability of the inverter.

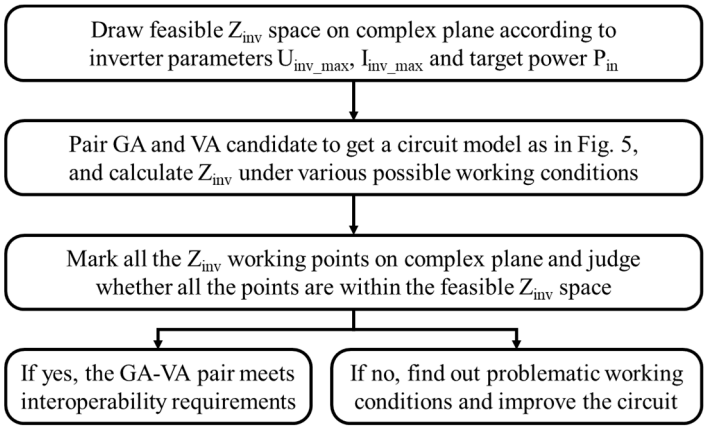

Figure 8. Interoperability evaluation for GA and VA candidate using Z_{inv}.

3.3. Interoperability Evaluation Index II: Z_S/Z_P

The power Equation (9) indicates that when diverse GAs and VAs are paired, the coil currents could change due to variation in circuit topology and parameters, even if the target power does not change. As a result, GA and VA coil currents may exceed their limit. Based on this fact, the role of Z_S/Z_P is to convert current limitations of GA and VA coils into safe impedance area of the circuit. An important difference between the two evaluation indices is that the feasible space of Z_{inv} is completely determined by GA, whereas the feasible space of Z_S/Z_P is determined by GA and VA together.

Assume that the maximum currents of GA and VA coils are I_{P_max} and $I_{S_max,}$ respectively.

$$|I_P| \le I_{P_max},\ |I_S| \le I_{S_max}. \tag{15}$$

According to Kirchhoff's voltage law,

$$\dot{I}_P Z_P + \dot{I}_S Z_S = 0. \tag{16}$$

Hence,

$$|I_P|/|I_S| = |Z_S/Z_P|,\ \varphi(I_P, I_S) = -\varphi(Z_S/Z_P), \tag{17}$$

where $|Z_S/Z_P|$ and $\varphi(Z_S/Z_P)$ are the amplitude and phase of Z_S/Z_P.

The transmission power can be expressed as

$$\begin{aligned} P &= \omega M|I_P||I_S|\sin\varphi(I_P, I_S) \\ &= \omega M|I_S|^2|Z_S/Z_P|\sin(-\varphi(Z_S/Z_P)) \\ &= \frac{\omega M|I_P|^2\sin(-\varphi(Z_S/Z_P))}{|Z_S/Z_P|} \end{aligned} \tag{18}$$

From Equations (15) and (18), the amplitude constraints of Z_S/Z_P are derived:

$$\max|Z_S/Z_P| = \frac{\omega M I_{P_max}^2 \sin(-\varphi(Z_S/Z_P))}{P},\ \min|Z_S/Z_P| = \frac{P}{\omega M I_{S_max}^2 \sin(-\varphi(Z_S/Z_P))}. \tag{19}$$

From Equation (19), the feasible impedance space of Z_S/Z_P is determined, and it can also be transformed into the complex plane, as shown in Figure 9.

Figure 10 shows the steps of interoperability evaluation using Z_S/Z_P, which is similar to Figure 8. The main difference is that Z_S/Z_P evaluates the power capability of the GA-VA coil pair. In addition, it is recommended that the evaluation process should be carried out twice, i.e., M_{max} case and M_{min} case.

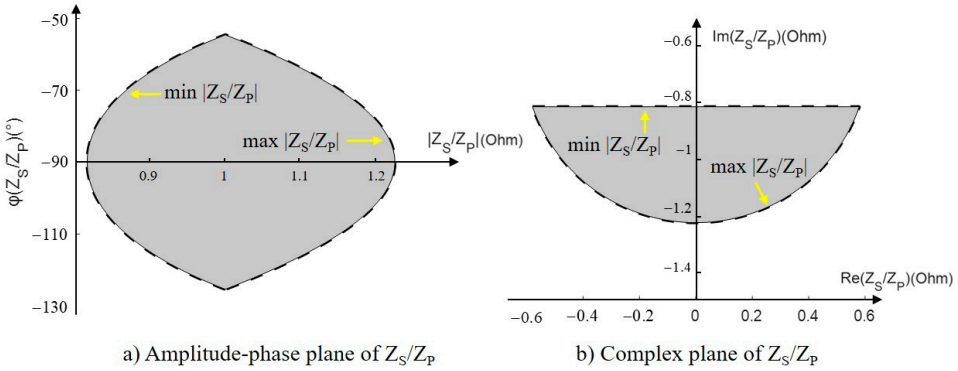

a) Amplitude-phase plane of Z_S/Z_P b) Complex plane of Z_S/Z_P

Figure 9. An example of feasible Z_S/Z_P space.

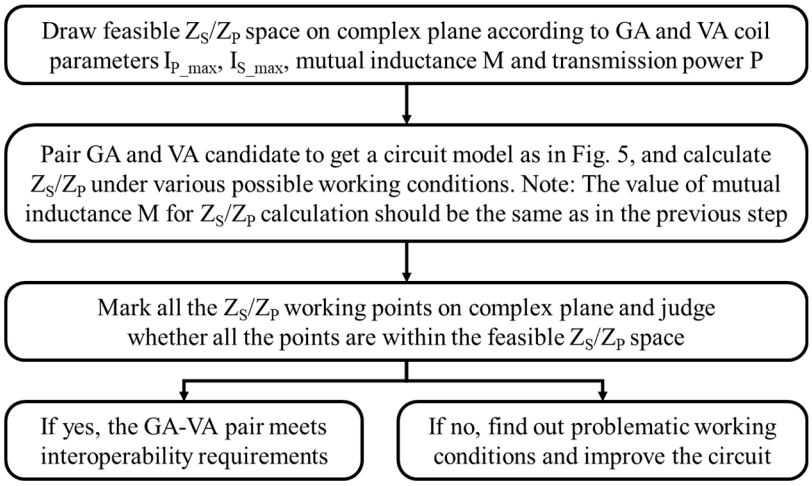

Figure 10. Interoperability evaluation for the GA and VA candidate using Z_S/Z_P.

4. Interoperability Evaluation Based on Chinese WEVC Standard

In the Chinese standard for WEVC, a set of reference devices is developed with the aim to test the interoperability of market-developed devices. The reference devices include one reference GA applied to all power and ground clearance levels (WPT1~WPT3, Z1~Z3), and nine reference VAs for WPT1~WPT3, Z1~Z3, respectively [3,4]. If the market-developed device can pair up with reference devices and achieve safe charging at expected power and relative positions, it will pass the interoperability test and get market access.

However, the interoperability test between reference devices and market-developed devices requires a large cost, so it is generally carried out after the design stage. As a result, the interoperability test can hardly help improve the design of market-developed devices. This section will apply the interoperability evaluation method to reference devices, so that R&D engineers of WEVC could use it to evaluate the interoperability between their devices and reference devices, and improve their design at the early stage.

4.1. Feasible Impedance Space of Reference Devices

The double-sided LCC compensation topology is adopted in the reference devices of Chinese standard due to its good performance. The circuit diagram is shown in Figure 11, and the current and voltage limits are listed in Table 3.

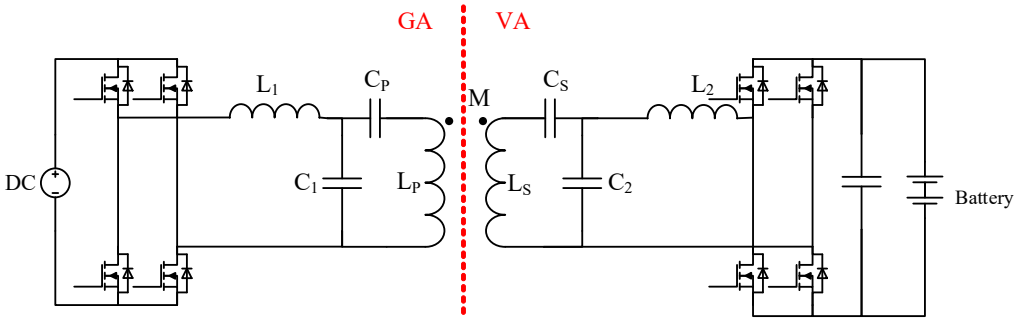

Figure 11. Reference GA-VA circuit.

Table 3. Current and voltage limits of reference devices.

	WPT1	WPT2	WPT3
U_{inv_max}	840 V	840 V	840 V
I_{inv_max}	45 A	45 A	45 A
I_{P_max}	65 A	65 A	65 A
I_{S_max}	35 A	50 A	75 A

By using the method introduced in Section 3.2. and substituting the data in Table 3 into the equations, the feasible Z_{inv} space can be obtained, as displayed in Figure 12. The feasible Z_{inv} space of WPT1~WPT3 appears as a similar shape, which is a part of a circle. As the power level increases, the feasible space shrinks significantly.

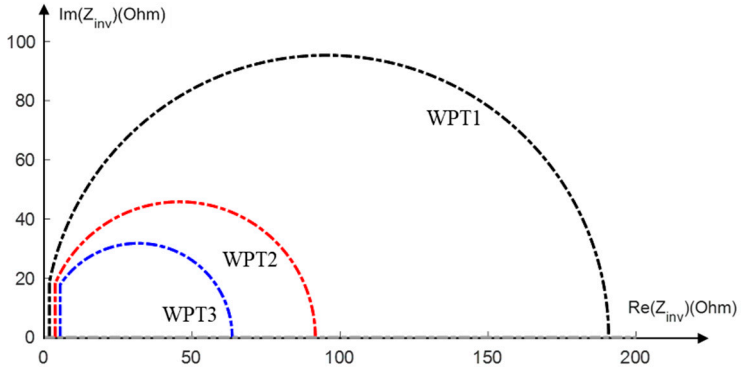

Figure 12. Feasible impedance space of Z_{inv} under different power levels.

Similarly, the feasible Z_S/Z_P space can also be obtained based on Equation (19). Note that different mutual inductances result in different feasible Z_S/Z_P space, so the feasible Z_S/Z_P spaces at Z1(M_{max}, M_{min}), Z2(M_{max}, M_{min}), Z3(M_{max}, M_{min}) are displayed separately. In addition, transmission power is also involved in Equation (19). The feasible Z_S/Z_P spaces are displayed in Figure 13. They all appear a shape of circular segment. The increase of power and the decrease of mutual inductance lead to a decrease in the area of the feasible space.

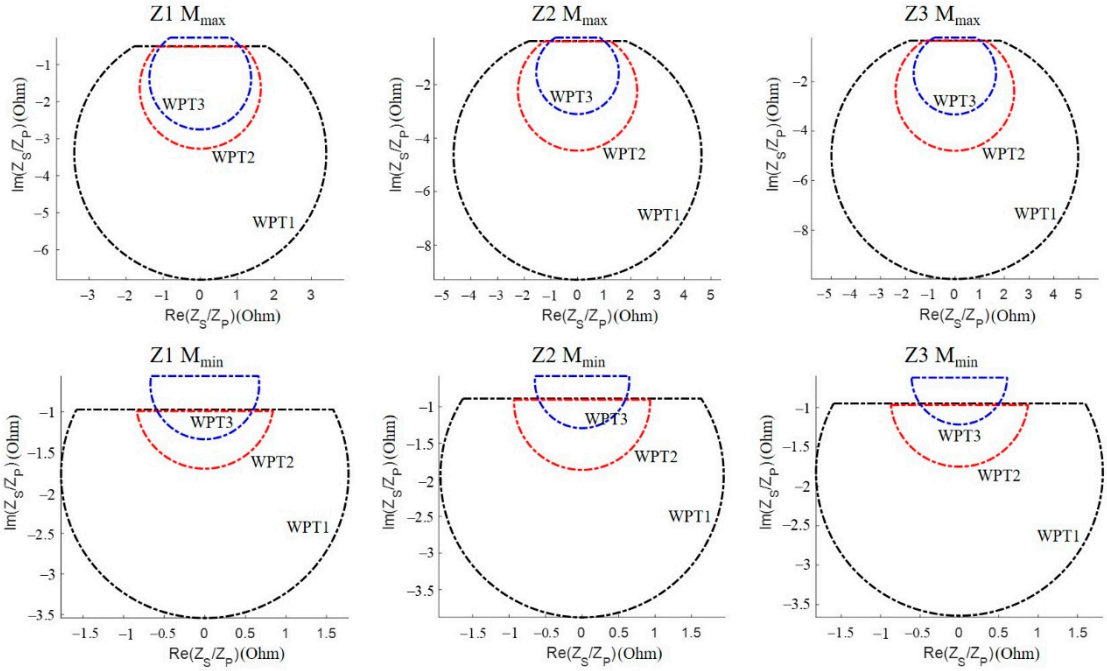

Figure 13. Feasible impedance space of Z_S/Z_P under different power and ground clearance levels.

4.2. An Application Example: Evaluate Interoperability between Reference GA and VA

As a reference device for interoperability test, the reference GA-VA pair is supposed to be interoperable. Therefore, the Z_{inv} and Z_S/Z_P points of the reference GA-VA pair should be within their corresponding regions. In the following part, the impedance points will be calculated according to the circuit parameters and test conditions published in the standard.

Since the parameters of the compensation network have been listed in the standard documents, it will not be repeated here. It is worth mentioning that the battery load and rectifier can be regarded as a load resistance, and its value depends on the operating condition of battery and rectifier. As stated in the standard document, the battery voltage range is set to 320~450 V. Assuming that the duty cycle of the rectifier D = 100% regardless of whether the battery voltage is at the maximum or minimum, and the load resistances are:

$$R_L = \frac{\left(\frac{2\sqrt{2}}{\pi} U_{bat_min}\right)^2}{P_{out}} \text{ at } U_{bat_min},\ D = 100\%, \tag{20}$$

$$R_L = \frac{\left(\frac{2\sqrt{2}}{\pi} U_{bat_max}\right)^2}{P_{out}} \text{ at } U_{bat_max},\ D = 100\%. \tag{21}$$

Accordingly, the impedance points of reference GA-VA pair are scattered over the impedance space, as shown in Figures 14–17.

Figures 14 and 15 are Z_{inv} and Z_S/Z_P points at minimum battery voltage. It can be found that all Z_{inv} and Z_S/Z_P points are within their feasible range at corresponding power levels, except that a Z_S/Z_P point at WPT3/Z1 (M_{min}) is out of the range slightly. The out-of-range point means when the reference GA-VA pair (WPT3/Z1) operates at minimum battery voltage and minimum coupling position, the GA coil current I_P can exceed its limit slightly (3% estimated). Fortunately, the current margin of coil will ensure the normal operation of the system.

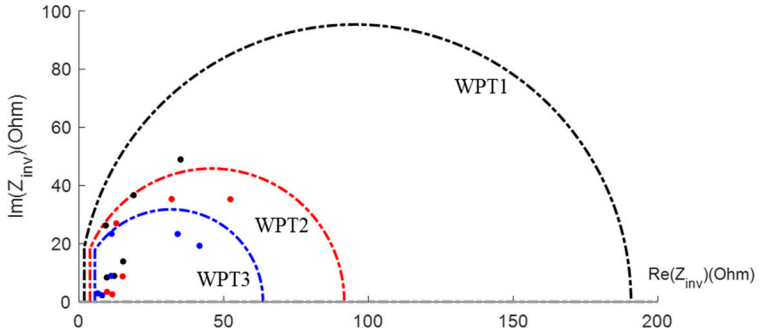

Figure 14. Z_{inv} operating points of reference GA-VA system (U_{bat_min}, D = 100%).

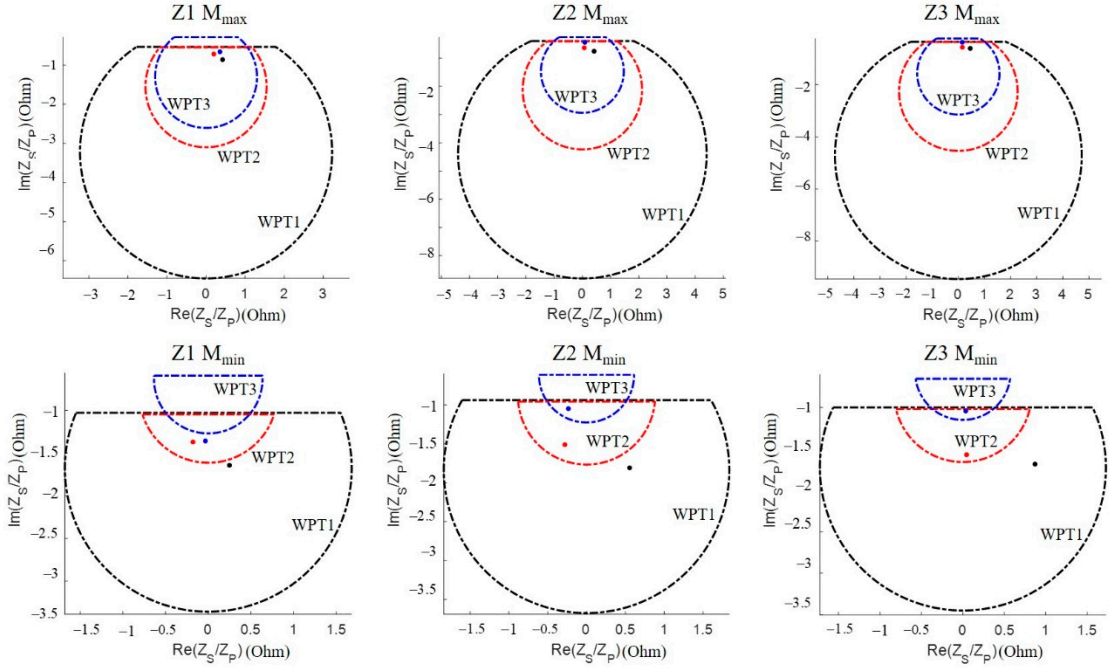

Figure 15. Z_S/Z_P operating points of reference GA-VA system (U_{bat_min}, D = 100%).

Figures 16 and 17 are Z_{inv} and Z_S/Z_P points at maximum U_{bat} and 100% rectifier duty cycle. There are 2/18 Z_{inv} points and 16/18 Z_S/Z_P points out of range. This result indicates that as the battery voltage rises, if the controller does not regulate down the duty cycle of rectifier, Z_{inv} and Z_S/Z_P will deviate from the ideal operating state, and cause voltages and currents to exceed the safe range.

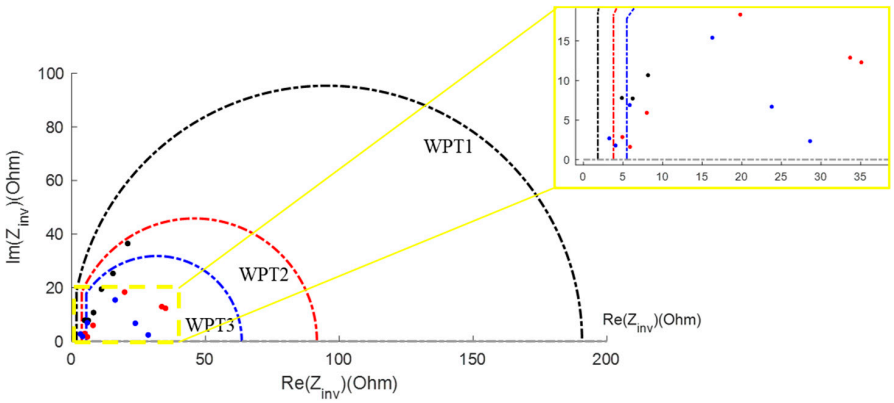

Figure 16. Z_{inv} operating points of reference GA-VA system (U_{bat_max}, D = 100%).

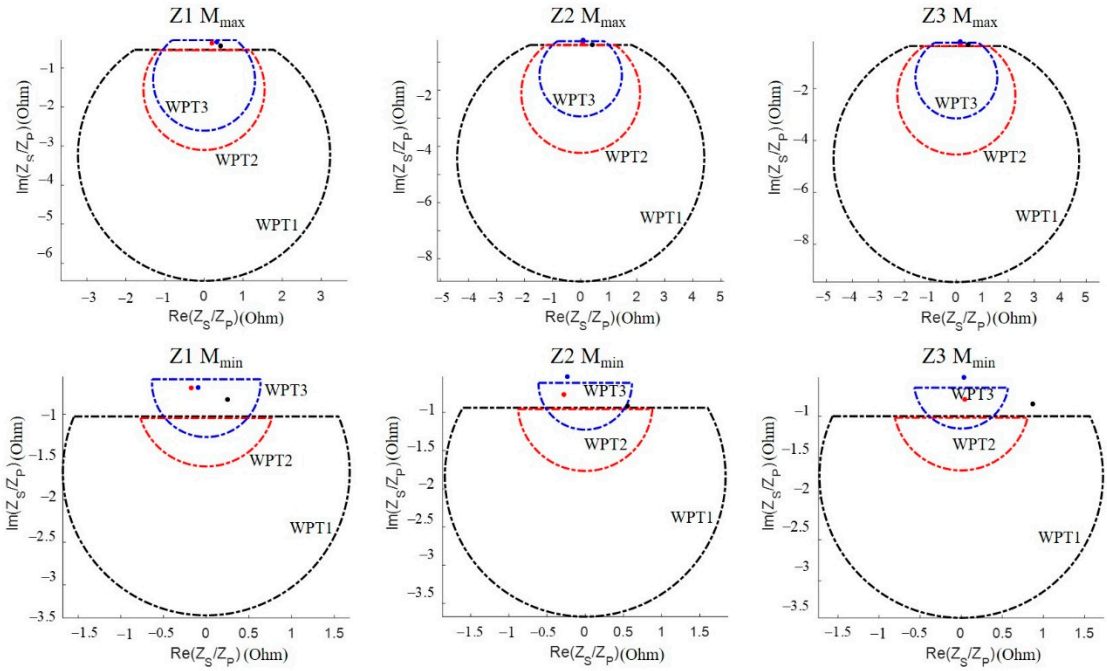

Figure 17. Z_S/Z_P operating points of reference GA-VA system (U_{bat_max}, D = 100%).

As the battery voltage rises, reducing the duty cycle can narrow down the variation of load resistance, so that the Z_{inv} and Z_S/Z_P points can get closer to minimum U_{bat} situation. Figures 18 and 19 are Z_{inv} and Z_S/Z_P points at maximum U_{bat} and 56% rectifier duty cycle. Under such conditions the load resistance is

$$R_L = \frac{\left(\frac{2\sqrt{2}}{\pi}\sin\left(0.56\cdot\frac{\pi}{2}\right)U_{bat_max}\right)^2}{P_{out}} \text{ at } U_{bat_max},\ D = 56\%. \quad (22)$$

The figures show that all points return to their feasible range.

This analysis proves the significance of introducing a controlled rectifier into the WEVC system. It also proves that the reference devices provided by Chinese standard are able to achieve the requirements of power capability.

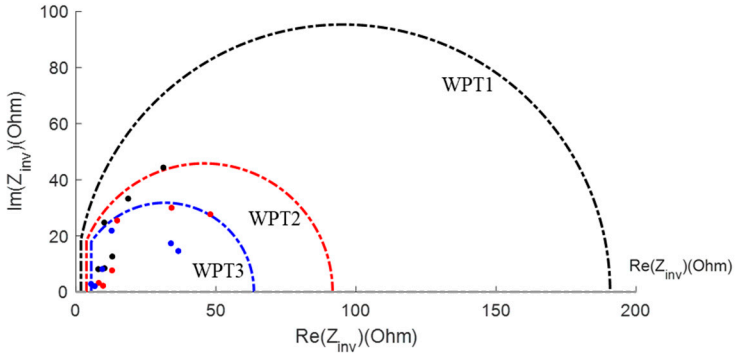

Figure 18. Z_{inv} operating points of reference GA-VA system (U_{bat_max}, D = 56%).

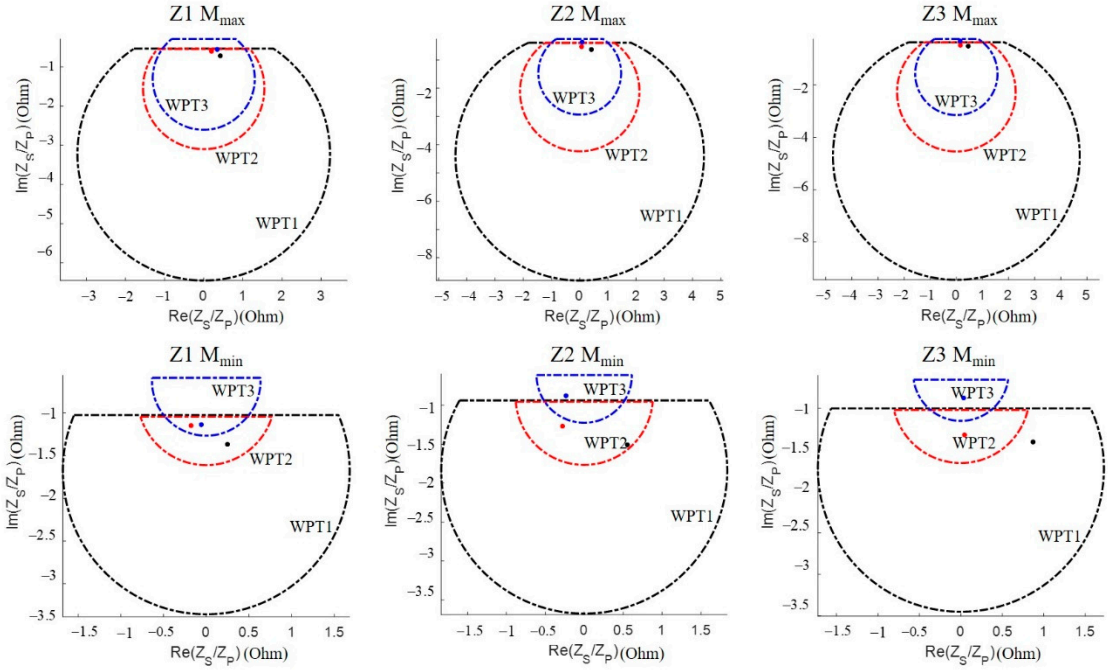

Figure 19. Z_S/Z_P operating points of reference GA-VA system (U_{bat_max}, D = 56%).

Full power tests are conducted to demonstrate the interoperability of the reference GA and VA devices. Table 4 lists the output power achieved in the lab, including all power and ground clearance levels. The tests cover the extremum of coupling conditions and battery voltages, and all results show sufficient power capability.

Table 4. Full power interoperability test data.

Power Class	Z Class	M_{max}, U_{bat_min}		M_{max}, U_{bat_max}		M_{min}, U_{bat_min}		M_{min}, U_{bat_max}	
		U_{bat}(V)	P_{bat}(kW)	U_{bat}(V)	P_{bat}(kW)	U_{bat}(V)	P_{bat}(kW)	U_{bat}(V)	P_{bat}(kW)
WPT1	Z1	320.1	3.25	451.4	3.31	320.2	3.25	450.9	3.30
	Z2	319.8	3.24	449.7	3.28	320.5	3.26	449.9	3.29
	Z3	320.8	3.27	450.3	3.30	321.3	3.27	450.8	3.30
WPT2	Z1	321.4	6.57	451.1	6.49	319.7	6.51	449.3	6.47
	Z2	319.5	6.62	447.2	6.64	319.7	6.62	446.7	6.62
	Z3	319.7	6.49	452.1	6.55	319.2	6.48	452.4	6.53
WPT3	Z1	319.6	10.03	449.5	10.02	319.5	10.02	449.6	9.97
	Z2	319.5	9.92	451.5	9.93	321.7	10.06	447.9	9.75
	Z3	319.3	9.91	451.3	10.02	321.5	10.03	449.1	9.83

5. Conclusions and Discussions

A wireless electric vehicle charging system includes coils, compensation networks, and converters. No matter what coil configurations and compensation topologies are adopted, the coil system can be regarded as a storage and transmission system of electromagnetic energy. Two types of energy are stored dynamically in the system, including the energy of self-induced flux and energy of mutual induced flux. The former flows in to one side of the coil, whereas the latter flows through both sides and transfer power from one to the other. Accordingly, frequency, amplitudes, and phase difference of coil currents, as well as the mutual inductance of coils are determinants of transmission power.

Various coil configurations and compensation topologies bring about the problem of interoperability, which means ground assemblies (GA) and vehicle assemblies (VA) can achieve a wireless power transmission that meets the performance and functional require-

ments, especially the power requirement. This paper proposes an electrical interoperability evaluation method based on two impedance indices. Z_{inv} is adopted to ensure the safety of the inverter, and Z_S/Z_P is adopted to make sure the coil currents are within their limits. Feasible ranges of Z_{inv} and Z_S/Z_P are obtained based on a set of reference devices in Chinese standard. The results of interoperability evaluation and experiments show that the reference devices are able to achieve the requirements of power capability. Moreover, it is necessary to reduce the duty cycle of the rectifier when the battery voltage rises so as to narrow down the variation of load resistance and avoid dangerous working conditions.

Supplementary Materials: The following are available online at https://www.mdpi.com/article/10.3390/wevj12040245/s1, experimental data of interoperability test.

Author Contributions: Conceptualization, B.S. and F.Y.; methodology, B.S. and F.Y.; software, B.S.; validation, B.W. and F.Y.; formal analysis, B.S.; investigation, B.S.; resources, B.W. and F.Y.; data curation, B.S.; writing—original draft preparation, B.S.; writing—review and editing, F.Y. and M.O.; visualization, B.S.; supervision, F.Y. and M.O.; project administration, F.Y.; funding acquisition, M.O. All authors have read and agreed to the published version of the manuscript.

Funding: This research was funded by the International Science and Technology Cooperation of China, grant number 2019YFE0100200.

Institutional Review Board Statement: Not applicable.

Informed Consent Statement: Not applicable.

Data Availability Statement: The data presented in this study are available in the supplementary material.

Conflicts of Interest: The authors declare no conflict of interest.

References

1. Bi, Z.; Kan, T.; Mi, C.; Zhang, Y.; Zhao, Z.; Keoleian, G.A. A review of wireless power transfer for electric vehicles: Prospects to enhance sustainable mobility. *Appl. Energy* **2016**, *179*, 413–425. [CrossRef]
2. National Technical Committee of Auto Standardization. *Electric Vehicle Wireless Power Transfer—Part 1: General Requirements*; GB/T 38775.1-2020; Standards Press of China: Beijing, China, 2020.
3. China Electricity Council. *Electric Vehicle Wireless Power Transfer—Part 3: Specific Requirements*; GB/T 38775.3-2020; Standards Press of China: Beijing, China, 2020.
4. China Electricity Council. *Electric Vehicle Wireless Power Transfer—Part 6: Interoperability Requirements and Testing—Ground Side*; GB/T 38775.6-2021; Standards Press of China: Beijing, China, 2021.
5. National Technical Committee of Auto Standardization. *Electric Vehicle Wireless Power Transfer—Part 7: Interoperability Requirements and Testing—Vehicle Side*; GB/T 38775.7-2021; Standards Press of China: Beijing, China, 2021.
6. Hybrid-EV Committee. *Wireless Power Transfer for Light-Duty Plug-In/Electric Vehicles and Alignment Methodology*; SAE TIR J2954_202010; SAE International: New York, NY, USA, 2020.
7. Shevchenko, V.; Husev, O.; Strzelecki, R.; Pakhaliuk, B.; Poliakov, N.; Strzelecka, N. Compensation Topologies in IPT Systems: Standards, Requirements, Classification, Analysis, Comparison and Application. *IEEE Access* **2019**, *7*, 120559–120580. [CrossRef]
8. Rim, C.T.; Mi, C. *Wireless Power Transfer for Electric Vehicles and Mobile Devices*; John Wiley & Sons: Hoboken, NJ, USA, 2017.
9. Chen, K.; Zhao, Z.; Liu, F.; Yuan, L. Analysis of Resonant Topology for Bi-directional Wireless Charging of Electric Vehicle. *Autom. Electr. Power Syst.* **2017**, *41*, 66–72.
10. Ramezani, A.; Farhangi, S.; Iman-Eini, H.; Farhangi, B.; Rahimi, R.; Moradi, G.R. Optimized LCC-Series Compensated Resonant Network for Stationary Wireless EV Chargers. *IEEE Trans. Ind. Electron.* **2019**, *66*, 2756–2765. [CrossRef]
11. Mai, R.; Chen, Y.; Zhang, Y.; Yang, N.; Cao, G.-Z.; He, Z. Optimization of the Passive Components for an S-LCC Topology-Based WPT System for Charging Massive Electric Bicycles. *IEEE Trans. Ind. Electron.* **2018**, *65*, 5497–5508. [CrossRef]
12. Schneider, J.; Kamichi, K.; Mikat, D.; Sutton, R.; Abdul-Hak, M.; Minagawa, Y.; Abeta, H.; Taha, E.; Boyer, R.; Sirota, J.; et al. Bench Testing Validation of Wireless Power Transfer up to 7.7 kW Based on SAE J2954. *SAE Int. J. Passeng. Cars-Electron. Electr. Syst.* **2018**, *11*, 89–108. [CrossRef]
13. Schneider, J.; Carlson, R.; Sirota, J.; Sutton, R.; Taha, E.; Kesler, M.; Kamichi, K.; Teerlinck, I.; Abeta, H.; Minagawa, Y.; et al. *Validation of Wireless Power Transfer up to 11 kW Based on SAE J2954 with Bench and Vehicle Testing*; SAE Technical Paper; SAE International: New York, NY, USA, 2019.